DRAFT VERSION MAY 21, 2021
Typeset using LaTeX **twocolumn** style in AASTeX63

A 30 Million Year Old Mini-Neptune in the Kepler Field

L. G. BOUMA[1] AND J. L. CURTIS[2,3]

[1]*Department of Astrophysical Sciences, Princeton University, 4 Ivy Lane, Princeton, NJ 08540, USA*
[2]*Department of Astronomy, Columbia University, 550 West 120th Street, New York, NY 10027, USA*
[3]*Department of Astrophysics, American Museum of Natural History, Central Park West, New York, NY 10024, USA*

(Received —; Revised —; Accepted —)

Submitted to Nature

ABSTRACT

The Gaia satellite is revitalizing our understanding of nearby open clusters and moving groups. Here, we focus on the underappreciated δ Lyr cluster. Based on rotation periods from TESS and lithium measurements from ground-based spectrographs, we find the age of the cluster to be $30 \pm XX$ Myr. Kepler 1627 is a binary system in the cluster, serendipitously observed by the Kepler satellite because the primary is nearby and Sun-like. Kepler 1627A was previously found to host a $3.56 \pm 0.04 R_\oplus$ mini-Neptune on a 7.2 day orbit. We re-validate the existence of Kepler 1627Ab, cementing it as the youngest planet with a well-measured age observed by the main Kepler mission. Newly derived ages from Gaia offer the opportunity to significantly expand the census of age-dated planets – we offer a literature compilation of young stars to enable this expansion. The properties of Kepler 1627Ab are may also help clarify how the orbits and atmospheres of the mini-Neptune planets evolve.

Keywords: planetary evolution (XXXX), stellar associations (1582), open star clusters (1160), stellar ages (1581),

1. INTRODUCTION

At the time of the main Kepler mission (2009–2013), only four open clusters were known in the Kepler field: NGC 6866, NGC 6811, NGC 6819, and NGC 6791, with ages spanning 0.7 Gyr to 9 Gyr (Meibom et al. 2011).

Section 2. Section 3. In Section 4, we discuss. Section 5 gives our conclusions.

2. FIRST

3. SECOND

The models were fitted using exoplanet...

4. DISCUSSION

5. CONCLUSION

ACKNOWLEDGMENTS

L.G.B. and J.L.C. are grateful to T. David for help with the transit fitting. L.G.B. acknowledges support by the TESS GI Program, programs G011103 and G022117, through NASA grants 80NSSC19K0386 and 80NSSC19K1728. L.G.B. was also supported by a Charlotte Elizabeth Procter Fellowship from Princeton University. This study was based in part on observations at Cerro Tololo Inter-American Observatory at NSF's NOIRLab (NOIRLab Prop. ID 2020A-0146; 2020B-0029 PI: Bouma), which is managed by the Association of Universities for Research in Astronomy (AURA) under a cooperative agreement with the National Science Foundation. This paper also includes data collected by the TESS mission, which are publicly available from the Mikulski Archive for Space Telescopes (MAST). Funding for the TESS mission is provided by NASA's Science Mission directorate. We thank the TESS Architects (G. Ricker, R. Vanderspek, D. Latham, S. Seager, J. Jenkins) and the many TESS team members for their efforts to make the mission a continued success.

Software: `astrobase` (Bhatti et al. 2018), `astropy` (Astropy Collaboration et al. 2018), `astroquery` (Ginsburg et al. 2018), `corner` (Foreman-Mackey 2016), `exoplanet` (Foreman-Mackey et al. 2020), and its dependencies (Agol et al. 2020; Kipping 2013; Luger et al. 2019; Theano Development Team 2016), `IPython` (Pérez & Granger 2007), `matplotlib` (Hunter 2007), `numpy` (Walt et al. 2011), `pandas` (McKinney 2010), `PyMC3` (Salvatier et al. 2016), `scipy` (Jones et al. 2001), `TESS-point` (Burke et al. 2020), `wotan` (Hippke et al. 2019).

Corresponding author: L. G. Bouma
luke@astro.princeton.edu

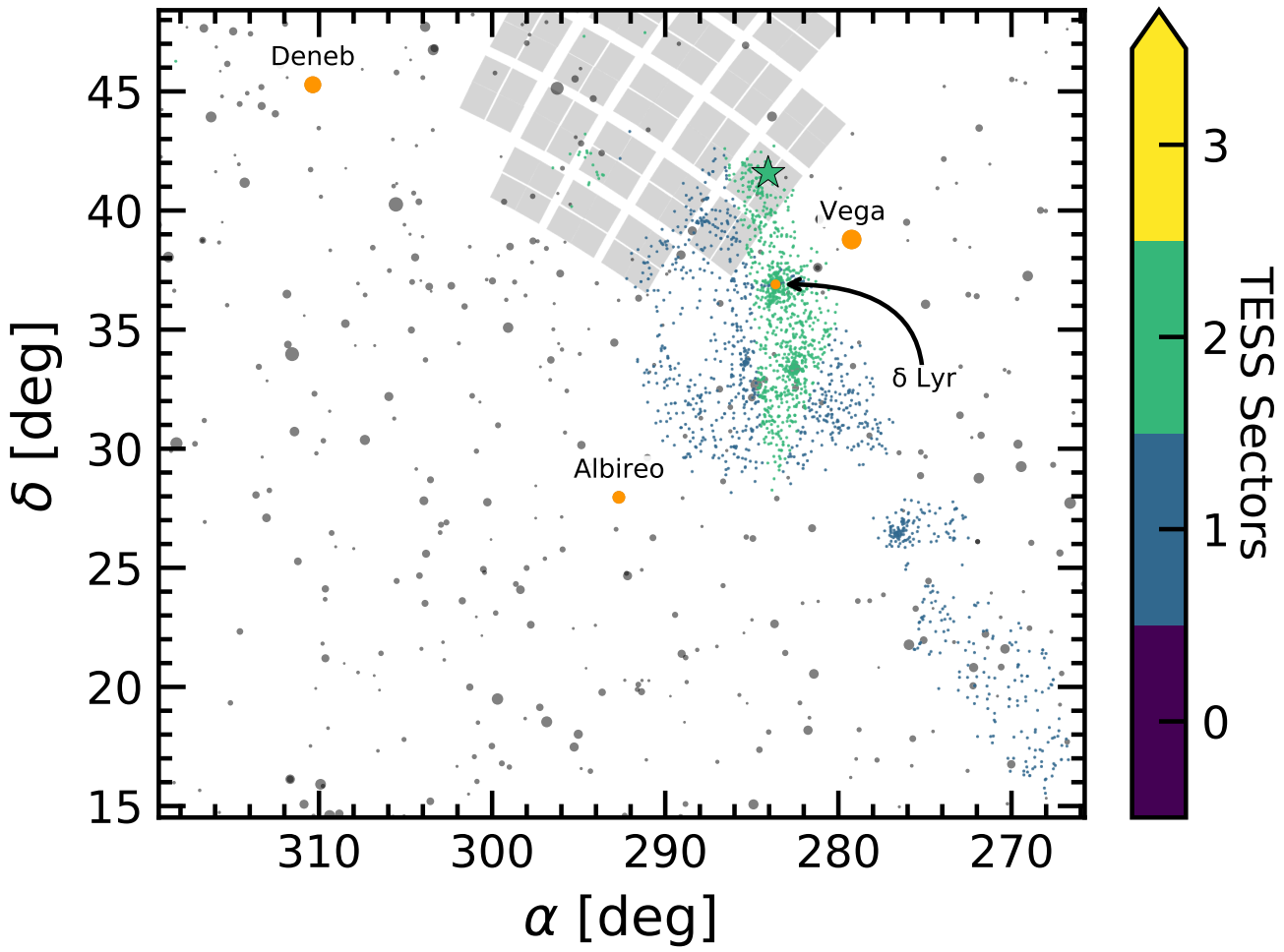

Figure 1. Kepler and TESS views of the δ Lyr cluster. Colored points are kinematically selected members of the δ Lyr cluster (black points in Figure 4). Both Kepler (gray panels) and TESS (colored points) observed portions of the cluster. Naked-eye stars ($m_V < 6.5$) are shown in gray; four of them (orange points) have their names shown. Kepler 1627 (green star) was observed during the entirety of the Kepler mission, and has been observed by TESS for two lunar months to date.

Facilities: *Astrometry*: Gaia (Gaia Collaboration et al. 2018b, 2020). *Imaging*: Second Generation Digitized Sky Survey. *Spectroscopy*: CTIO1.5 m (CHIRON; Tokovinin et al. 2013), AAT (HERMES; Lewis et al. 2002; Sheinis et al. 2015), VLT:Kueyen (FLAMES; Pasquini et al. 2002). *Photometry*: TESS (Ricker et al. 2015).

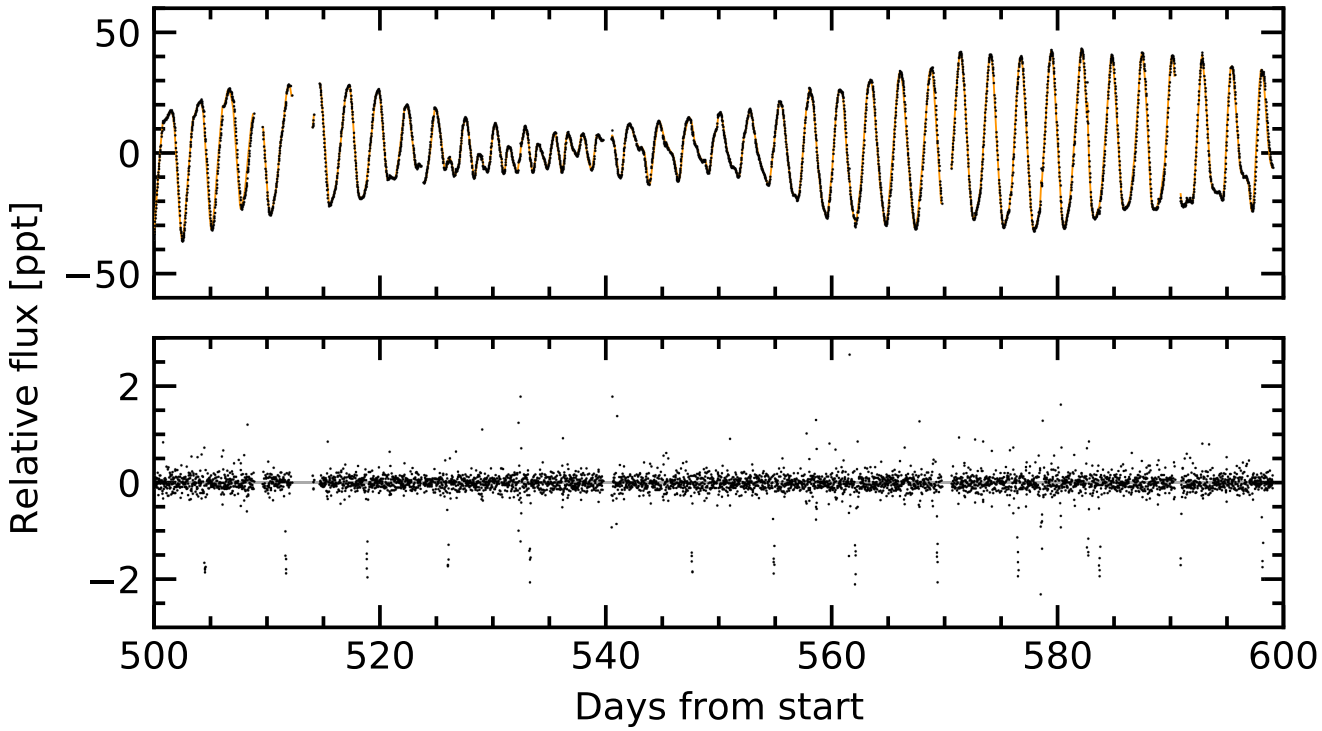

Figure 2. Kepler 1627 light curve over 100 days. The full Kepler dataset spans 1,437 days (3.9 years), sampled at 30 minute cadence. The *top panel* shows the `PDCSAP` median-subtracted flux in units of parts-per-thousand ($\times 10^{-3}$). The dominant signal is induced by starspots and plages. The model for the stellar variability (orange line) is subtracted in the *bottom panel*, revealing the transits of Kepler 1627Ab, as well as other deviations from the stellar variability model. The Figure Set available online shows the entire 3.9 years of available data.

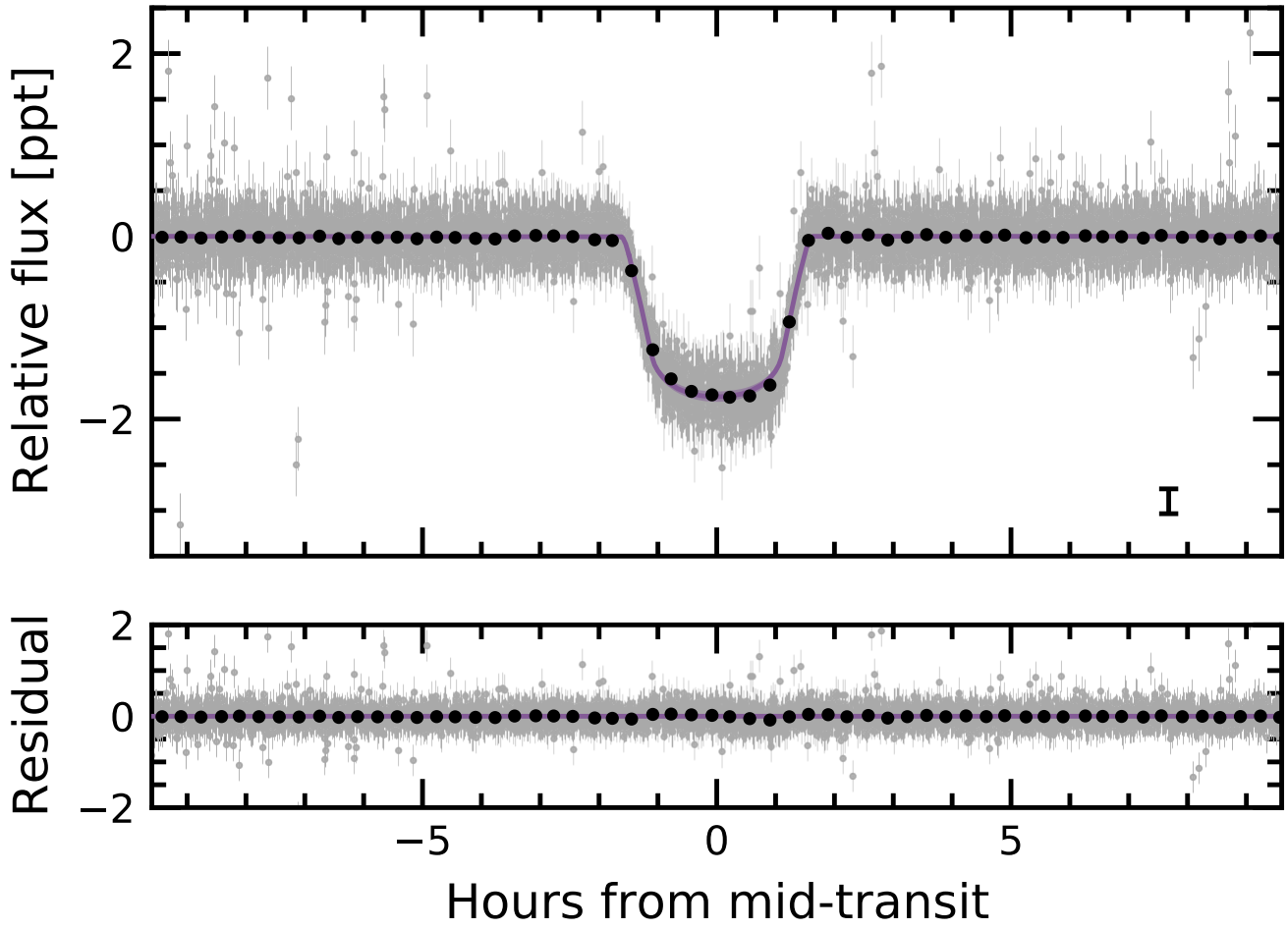

Figure 3. Phase-folded transit of Kepler 1627b, with stellar variability removed. The 1-σ model uncertainties and the median model are shown as the faint purple band, and the dark purple line. Gray points are individual `PDCSAP` flux measurements; black points are binned to 20 minutes, with a representative error bar shown.

Table 1. Priors and posteriors for the transit and stellar variability model fitted to the long-cadence Kepler 1627b photometric timeseries.

Param.	Unit	Prior	Median	Mean	Std. Dev.	3%	97%	ESS	$\hat{R}-1$
Sampled									
P	d	$\mathcal{N}(7.20281; 0.01000)$	7.202804	7.202804	0.0000072	7.2027906	7.2028173	2562.0012087	0.0011528
$t_0^{(1)}$	d	$\mathcal{N}(120.79053; 0.02000)$	120.7903359	120.7903263	0.0009056	120.7886253	120.7920160	1982.4196452	0.0000234
$\log R_p/R_\star$	–	$\mathcal{U}(-4.605; 0.000)$	-3.3349	-3.33418	0.06621	-3.46662	-3.21543	1203.15584	0.0038
b	–	$\mathcal{U}(0; 1+R_p/R_\star)$	0.3648	0.3623	0.2083	0.0001	0.6914	226.4445	0.0064
u_1	–	$\mathcal{U}(0.310; 0.710)$	0.393	0.406	0.072	0.310	0.538	1058.579	0.007
u_2	–	$\mathcal{U}(0.040; 0.440)$	0.218	0.223	0.110	0.041	0.401	1201.271	-0.
$R_\star$	$R_\odot$	$\mathcal{T}(0.910; 0.052)$	0.911	0.910	0.052	0.812	1.002	2132.132	0.001
$\log g$	cgs	$\mathcal{N}(4.600; 0.100)$	4.617	4.610	0.095	4.433	4.775	1074.583	0.002
$\langle f \rangle$	–	$\mathcal{N}(1.000; 0.100)$	0.4999	0.4999	0.0007	0.4986	0.5014	2324.6122	0.0025
$e^{(2)}$	–	Van Eylen et al. (2019)	0.124	0.167	0.151	0.	0.440	674.320	0.003
ω	rad	$\mathcal{U}(0.000; 6.283)$	-0.181	-0.144	1.932	-3.137	2.9	931.911	-0.001
$\log \sigma_f$	–	$\mathcal{N}(\log\langle\sigma_f\rangle; 2.000)$	-8.058	-8.058	0.007	-8.072	-8.045	1865.285	0.002
ρ	d	InvGamma(0.500; 2.000)	4.317	4.320	0.138	4.071	4.579	2112.469	0.
σ	d^{-1}	InvGamma(1.000; 5.000)	0.026	0.026	0.001	0.024	0.028	2177.477	0.
σ_{rot}	d^{-1}	InvGamma(1.000; 5.000)	0.662	0.681	0.136	0.452	0.940	1703.701	0.002
$\log P_{rot}$	log(d)	$\mathcal{N}(0.958; 0.020)$	1.66	1.66	0.002	1.656	1.663	2494.624	0.
$\log Q_0$	–	$\mathcal{N}(0.000; 2.000)$	10.514	10.551	0.662	9.383	11.832	479.465	0.008
$\log dQ$	–	$\mathcal{N}(0.000; 2.000)$	15.963	15.973	0.769	14.425	17.350	1432.296	0.
f	–	$\mathcal{U}(0.100; 1.000)$	0.201	0.324	0.259	0.1	0.877	295.040	0.013
Derived									
$R_p/R_\star$	–	–	0.036	0.036	0.002	0.031	0.040	1203.156	0.004
$\rho_\star$	g cm^{-3}	–	2.336	2.361	0.518	1.454	3.280	1079.762	0.002
R_p	R_{Jup}	–	0.316	0.317	0.038	0.245	0.385	1671.595	0.001
$a/R_\star$	–	–	18.572	18.539	1.370	15.859	20.798	1079.783	0.002
$\cos i$	–	–	0.02	0.02	0.011	0.	0.036	251.447	0.007
T_{14}	hr	–	2.815	2.817	0.048	2.727	2.908	883.771	0.001
T_{13}	hr	–	2.579	2.570	0.065	2.448	2.688	592.371	0.003

NOTE— ESS refers to the number of effective samples. $\hat{R}$ is the Gelman-Rubin convergence diagnostic. Logarithms through this table are in base-e. $\mathcal{U}$ denotes a uniform distribution, $\mathcal{N}$ a normal distribution, and $\mathcal{T}$ a truncated normal bounded between zero and an upper limit much larger than the mean. (1) The ephemeris is in units of BJDTDB - 2454833. (2) The eccentricity vectors are sampled in the $(e\cos\omega, e\sin\omega)$ basis.

REFERENCES

Agol, E., Luger, R., & Foreman-Mackey, D. 2020, AJ, 159, 123

Akeson, R. L., Chen, X., Ciardi, D., et al. 2013, PASP, 125, 989

Astropy Collaboration, Price-Whelan, A. M., Sipőcz, B. M., et al. 2018, AJ, 156, 123

Bhatti, W., Bouma, L. G., & Wallace, J. 2018, `astrobase`, https://doi.org/10.5281/zenodo.1469822

Boisse, I., Pepe, F., Perrier, C., et al. 2012, A&A, 545, A55

Bouma, L. G., Hartman, J. D., Bhatti, W., Winn, J. N., & Bakos, G. Á. 2019, ApJS, 245, 13

Burke, C. J., Levine, A., Fausnaugh, M., et al. 2020, TESS-Point: High precision TESS pointing tool, Astrophysics Source Code Library, ascl:2003.001

Cantat-Gaudin, T., & Anders, F. 2020, A&A, 633, A99

Cantat-Gaudin, T., Jordi, C., Vallenari, A., et al. 2018, A&A, 618, A93

Cantat-Gaudin, T., Jordi, C., Wright, N. J., et al. 2019, A&A, 626, A17

Cantat-Gaudin, T., Anders, F., Castro-Ginard, A., et al. 2020, A&A, 640, A1

Castro-Ginard, A., Jordi, C., Luri, X., et al. 2020, A&A, 635, A45

Cotten, T. H., & Song, I. 2016, ApJS, 225, 15

Damiani, F., Prisinzano, L., Pillitteri, I., Micela, G., & Sciortino, S. 2019, A&A, 623, A112

Dias, W. S., Monteiro, H., Caetano, T. C., et al. 2014, Astronomy and Astrophysics, 564, A79

Esplin, T. L., & Luhman, K. L. 2019, AJ, 158, 54

Foreman-Mackey, D. 2016, Journal of Open Source Software, 1, 24

Foreman-Mackey, D., Czekala, I., Luger, R., et al. 2020, exoplanet-dev/exoplanet v0.2.6

Fürnkranz, V., Meingast, S., & Alves, J. 2019, A&A, 624, L11

Gagné, J., David, T. J., Mamajek, E. E., et al. 2020, ApJ, 903, 96

Gagné, J., & Faherty, J. K. 2018, ApJ, 862, 138

Gagné, J., Roy-Loubier, O., Faherty, J. K., Doyon, R., & Malo, L. 2018a, ApJ, 860, 43

Gagné, J., Mamajek, E. E., Malo, L., et al. 2018b, ApJ, 856, 23

Gaia Collaboration, Brown, A. G. A., Vallenari, A., et al. 2020, arXiv e-prints, arXiv:2012.01533

Gaia Collaboration, Babusiaux, C., van Leeuwen, F., et al. 2018a, A&A, 616, A10

Gaia Collaboration, Brown, A. G. A., Vallenari, A., et al. 2018b, A&A, 616, A1

Ginsburg, A., Sipocz, B., Madhura Parikh, et al. 2018, Astropy/Astroquery: V0.3.7 Release

Goldman, B., Röser, S., Schilbach, E., Moór, A. C., & Henning, T. 2018, ApJ, 868, 32

Hippke, M., David, T. J., Mulders, G. D., & Heller, R. 2019, AJ, 158, 143

Hunter, J. D. 2007, Computing in Science & Engineering, 9, 90

Jones, E., Oliphant, T., Peterson, P., et al. 2001, Open source scientific tools for Python

Kharchenko, N. V., Piskunov, A. E., Schilbach, E., Röser, S., & Scholz, R.-D. 2013, A&A, 558, A53

Kipping, D. M. 2013, MNRAS, 435, 2152

Kounkel, M., & Covey, K. 2019, AJ, 158, 122

Kounkel, M., & Covey, K. 2019, AJ, 158, 122

Kounkel, M., Covey, K., & Stassun, K. G. 2020, AJ, 160, 279

Kounkel, M., Covey, K., Suárez, G., et al. 2018, AJ, 156, 84

Kounkel, M., Covey, K., Suárez, G., et al. 2018, AJ, 156, 84

Kraus, A. L., Shkolnik, E. L., Allers, K. N., & Liu, M. C. 2014, AJ, 147, 146

Lewis, I. J., Cannon, R. D., Taylor, K., et al. 2002, MNRAS, 333, 279

Luger, R., Agol, E., Foreman-Mackey, D., et al. 2019, AJ, 157, 64

Mann, A. W., Johnson, M. C., Vanderburg, A., et al. 2020, AJ, 160, 179

McKinney, W. 2010, in Proceedings of the 9th Python in Science Conference, ed. S. van der Walt & J. Millman, 51

Meibom, S., Barnes, S. A., Latham, D. W., et al. 2011, The Astrophysical Journal Letters, 733, L9

Meingast, S., & Alves, J. 2019, A&A, 621, L3

Meingast, S., Alves, J., & Rottensteiner, A. 2021, A&A, 645, A84

Oh, S., Price-Whelan, A. M., Hogg, D. W., Morton, T. D., & Spergel, D. N. 2017, AJ, 153, 257

Pasquini, L., Avila, G., Blecha, A., et al. 2002, The Messenger, 110, 1

Pavlidou, T., Scholz, A., & Teixeira, P. S. 2021, MNRAS, 503, 3232

Pérez, F., & Granger, B. E. 2007, Computing in Science and Engineering, 9, 21

Ratzenböck, S., Meingast, S., Alves, J., Möller, T., & Bomze, I. 2020, A&A, 639, A64

Ricker, G. R., Winn, J. N., Vanderspek, R., et al. 2015, Journal of Astronomical Telescopes, Instruments, and Systems, 1, 014003

Rizzuto, A. C., Mann, A. W., Vanderburg, A., Kraus, A. L., & Covey, K. R. 2017, AJ, 154, 224

Roccatagliata, V., Franciosini, E., Sacco, G. G., Randich, S., & Sicilia-Aguilar, A. 2020, A&A, 638, A85

Röser, S., & Schilbach, E. 2020, A&A, 638, A9

Salvatier, J., Wieckiâ, T. V., & Fonnesbeck, C. 2016, PyMC3: Python probabilistic programming framework

Sheinis, A., Anguiano, B., Asplund, M., et al. 2015, Journal of Astronomical Telescopes, Instruments, and Systems, 1, 035002

Theano Development Team. 2016, arXiv e-prints, abs/1605.02688

Tian, H.-J. 2020, ApJ, 904, 196

Tokovinin, A., Fischer, D. A., Bonati, M., et al. 2013, PASP, 125, 1336

Ujjwal, K., Kartha, S. S., Mathew, B., Manoj, P., & Narang, M. 2020, AJ, 159, 166

Van Eylen, V., Albrecht, S., Huang, X., et al. 2019, AJ, 157, 61

Villa Vélez, J. A., Brown, A. G. A., & Kenworthy, M. A. 2018, Research Notes of the American Astronomical Society, 2, 58

Walt, S. v. d., Colbert, S. C., & Varoquaux, G. 2011, Computing in Science & Engineering, 13, 22

Wenger, M., Ochsenbein, F., Egret, D., et al. 2000, A&AS, 143, 9

Zari, E., Hashemi, H., Brown, A. G. A., Jardine, K., & de Zeeuw, P. T. 2018, A&A, 620, A172

Table 2. Young, Age-dated, and Age-dateable Stars Within the Nearest Few Kiloparsecs (`v0.5` of the CDIPS Target List).

Parameter	Example Value	Description
`source_id`	1709456705329541504	Gaia DR2 source identifier.
`ra`	247.826	Gaia DR2 right ascension [deg].
`dec`	79.789	Gaia DR2 declination [deg].
`parallax`	35.345	Gaia DR2 parallax [mas].
`parallax_error`	0.028	Gaia DR2 parallax uncertainty [mas].
`pmra`	94.884	Gaia DR2 proper motion $\mu_\alpha \cos\delta$ [mas yr$^-$1].
`pmdec`	-86.971	Gaia DR2 proper motion μ_δ [mas yr$^-$1].
`phot_g_mean_mag`	6.85	Gaia DR2 G magnitude.
`phot_bp_mean_mag`	6.409	Gaia DR2 $G_{\rm BP}$ magnitude.
`phot_rp_mean_mag`	7.189	Gaia DR2 $G_{\rm RP}$ magnitude.
`cluster`	Uma,IR_excess,NASAExoArchive_ps_20210506	Comma-separated cluster or group name.
`age`	nan,nan,9.48	Comma-separated logarithm (base-10) of reported[a] age in years.
`mean_age`	9.48	Mean (ignoring NaNs) of `age` column.
`reference_id`	Ujjwal2020,CottenSong2016,NASAExoArchive_ps_20210506	Comma-separted provenance of group membership.
`reference_bibcode`	2020AJ....159..166U,2016ApJS..225...15C,2013PASP..125..989A	ADS bibcode corresponding to `reference_id`.

NOTE— Table 2 is published in its entirety in a machine-readable format. This table is a concatenation of the studies listed in Table 3. One entry is shown for guidance regarding form and content. In this particular example, the star has a cold Jupiter on a 16 year orbit, HD 150706b (Boisse et al. 2012). An infrared excess has been reported (Cotten & Song 2016), and the star was identified by Ujjwal et al. (2020) as a candidate UMa moving group member ($\approx$ 400 Myr; Mann et al. 2020). The star's RV activity and TESS rotation period corroborate its youth.

APPENDIX

A. YOUNG, AGE-DATED, AND AGE-DATEABLE STAR COMPILATION

The `v0.5` CDIPS target catalog (Table 2) includes some important updates from previous versions. As in Bouma et al. (2019), we collected membership information for young, age-dated, or age-dateable stars from across the literature. Table 3 gives a list of the sources included, and some brief summary statistics.

The first major important change is that the extent of analyses performed on the Gaia data at the time of our compilation was wide and deep enough that we opted to neglect pre-Gaia analyses, except in cases for which spectroscopically confirmed samples of stars had been collected. The membership lists for instance of Kharchenko et al. (2013) and Dias et al. (2014) (MWSC and DAML) were no longer required, especially given their relatively high field-star contamination rates compared to Gaia-derived membership catalogs.

For any of the catalogs for which Gaia DR2 identifiers were not immediately available, we either followed the spatial (plus proper-motion) crossmatching procedures described in Bouma et al. (2019), or else we pulled the Gaia DR2 source identifiers associated with the catalog from SIMBAD. We consequently opted to drop the `ext_catalog_name` and `dist` columns maintained in Bouma et al. (2019), as these were only populated for a small number of stars.

The most crucial parameters of a given star for our purposes are the Gaia DR2 source identifier (`source_id`), the cluster name (`cluster`), and the (`age`). Given the hierarchical nature of many stellar associations, we do not attempt to resolve the cluster names to a single unique string. The Orion complex for instance, can be divided into almost one hundred kinematic subgroups (Kounkel et al. 2018). Similar complexity applies to the problem of determining homogeneous ages, which we do not attempt to resolve. Instead, we simply merged the cluster names and ages reported by various authors together.

This means that our "age" column can be null, for cases in which the original authors did not report an age, and a reference literature age was not readily available. Nonetheless, since we do generally prefer stars with known ages, we made a few additional efforts to populate this column. When available, the age provenance is from the original analysis of the cluster. However, in a few cases we adopted other ages when the string-based crossmatches on the "cluster" name was straightforward. In particular, we used the ages determined by Cantat-Gaudin et al. (2020) to assign ages to the catalogs from Gaia Collaboration et al. (2018a), Cantat-Gaudin et al. (2018), Castro-Ginard et al. (2020), and Cantat-Gaudin & Anders (2020).

The catalogs we included for which ages were not immediately available were those of Cotten & Song (2016), Oh et al. (2017), Zari et al. (2018), Gagné et al. (2018b), Gagné et al. (2018a),Gagné & Faherty (2018), and Ujjwal et al. (2020). While in principle the moving group members discussed by Gagné et al. (2018b,a); Gagné & Faherty (2018) and Ujjwal et al. (2020) have easily associated ages, our SIMBAD cross-matching lost the moving group association from those studies, which should therefore be recovered tools such

Table 3. Provenances of Young and Age-Dateable Stars.

Reference	$N_{\rm Gaia}$	$N_{\rm Age}$	$N_{G_{\rm RP}<16}$
Kounkel et al. (2020)	987376	987376	775363
Cantat-Gaudin & Anders (2020)	433669	412671	269566
Cantat-Gaudin et al. (2018)	399654	381837	246067
Kounkel & Covey (2019)	288370	288370	229506
Cantat-Gaudin et al. (2020)	233369	227370	183974
Zari et al. (2018) UMS	86102	0	86102
Wenger et al. (2000) Y*?	61432	0	45076
Zari et al. (2018) PMS	43719	0	38435
Gaia Collaboration et al. (2018a) $d > 250$ pc	35506	31182	18830
Castro-Ginard et al. (2020)	33635	24834	31662
Wenger et al. (2000) Y*O	28406	0	16205
Villa Vélez et al. (2018)	14459	14459	13866
Cantat-Gaudin et al. (2019)	11843	11843	9246
Damiani et al. (2019) PMS	10839	10839	9901
Oh et al. (2017)	10379	0	10370
Meingast et al. (2021)	7925	7925	5878
Wenger et al. (2000) pMS*	5901	0	3006
Gaia Collaboration et al. (2018a) $d > 250$ pc	5378	817	3968
Kounkel et al. (2018)	5207	3740	5207
Ratzenböck et al. (2020)	4269	4269	2662
Wenger et al. (2000) TT*	4022	0	3344
Damiani et al. (2019) UMS	3598	3598	3598
Rizzuto et al. (2017)	3294	3294	2757
Akeson et al. (2013)	3107	868	3098
Tian (2020)	1989	1989	1394
Goldman et al. (2018)	1844	1844	1783
Cotten & Song (2016)	1695	0	1693
Gagné et al. (2018b)	1429	0	1389
Röser & Schilbach (2020) Psc-Eri	1387	1387	1107
Röser & Schilbach (2020) Pleiades	1245	1245	1019
Wenger et al. (2000) TT?	1198	0	853
Gagné & Faherty (2018)	914	0	913
Pavlidou et al. (2021)	913	913	504
Gagné et al. (2018a)	692	0	692
Ujjwal et al. (2020)	563	0	563
Gagné et al. (2020)	566	566	351
Esplin & Luhman (2019)	377	443	296
Roccatagliata et al. (2020)	283	283	232
Meingast & Alves (2019)	238	238	238
Fürnkranz et al. (2019) Coma-Ber	214	214	213
Fürnkranz et al. (2019) Neighbor Group	177	177	167
Kraus et al. (2014)	145	145	145

NOTE— Table 3 describes the provenances for the young and age-dateable stars in Table 2. $N_{\rm Gaia}$: number of Gaia stars we parsed from the literature source. $N_{\rm Age}$: number of stars in the literature source with ages reported. $N_{G_{\rm RP}<16}$: number of Gaia stars we parsed from the literature source with either $G_{\rm RP} < 16$, or a parallax S/N exceeding 5 and a distance closer than 100 pc. The latter criterion included a few hundred white dwarfs that would have otherwise been neglected. Some studies appear multiple times when multiple tables from the analysis were included in the concatenation.

as BANYAN Σ.[1]. We also included the SIMBAD object identifiers TT*, Y*O,Y*?, TT?, and pMS*. Finally, we also included every star in the NASA Exoplanet Archive ps table that had a Gaia identifier available (Akeson et al. 2013). If the age had finite uncertainties, we also included it, since stellar ages determined through the combination of isochrone-fitting and transit-derived stellar densities typically have higher precision than from isochrones alone.

The technical manipulations for the merging, cleaning, and joining were performed using pandas (McKinney 2010). The eventual crossmatch (using the Gaia DR2 source_id)

[1] http://www.exoplanetes.umontreal.ca/banyan/banyansigma.php

against the Gaia DR2 archive was performed asychronously on the Gaia archive website[2].

B. KINEMATIC SELECTION OF δ LYR CLUSTER MEMBERS

Figure 4 shows members of the δ Lyr cluster reported by Kounkel & Covey (2019) to be in the group. Galactic positions are determined and plotted only for stars with parallax signal-to-noise exceeding 20. The location of the Sun is shown on the plots. The non-uniform "clumps" might be an artifact of the data processing steps performed by Kounkel & Covey (2019). We therefore only consider stars in the immediate kinematic group around Kepler 1627. The tangential velocities relative to Kepler 1627 are shown in the bottom right panel. These are computed by assuming that every star has the same three-dimensional spatial velocity as Kepler 1627, where we assume a systemic radial velocity of -16.7 ± 0.2 km s^{-1} based on the reconnaissance spectra obtained by A. Howard on HIRES and D. Latham on TRES. The relevant projection effects are then taken into account, as discussed by *e.g.*, Meingast et al. (2021) and **L. Bouma et al (2021, submitted)**.

[2] https://gea.esac.esa.int/archive/

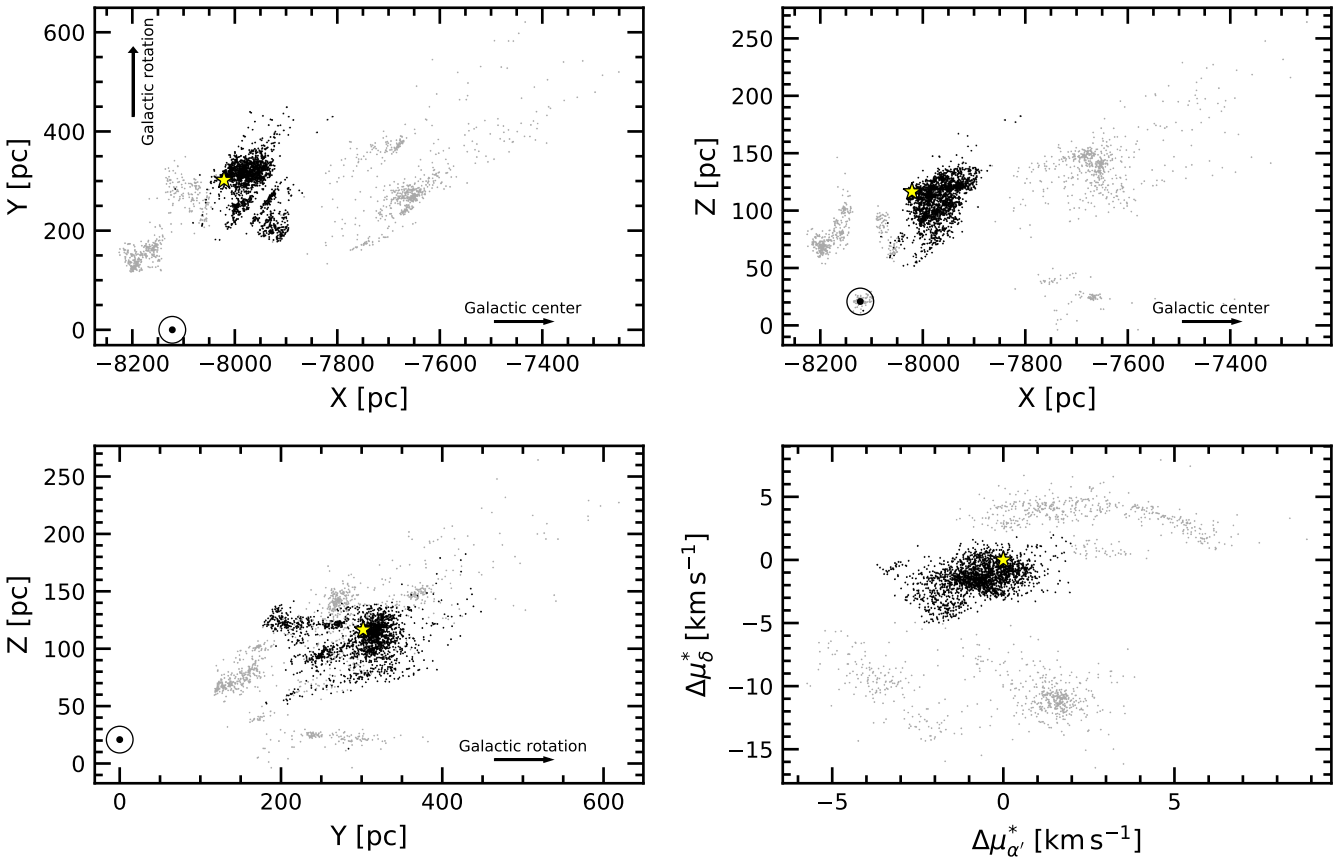

Figure 4. Galactic position and tangential velocities of the δ Lyr cluster (also known as Theia 73 and Stephenson 1). Points are candidate cluster members with $\varpi/\sigma_\varpi > 20$, reported to be in the group by Kounkel & Covey (2019). We focus on stars in a small region (black points) in the kinematic vicinity of Kepler 1627 (yellow star). The other candidate cluster members (gray points) may or may not share the ages of the selected kinematic group. The location of the Sun is ($\odot$) is shown.